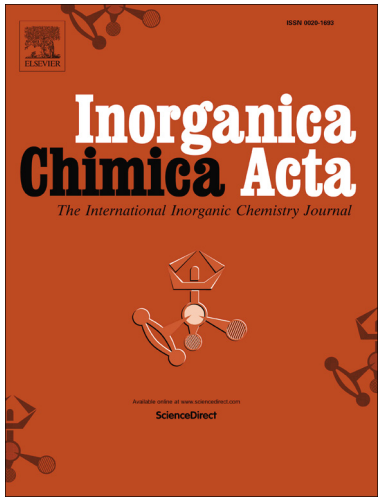

Hydrothermal synthesis and characterization of one dimensional chain structures of monolacunary Keggin polyoxoanions substituted with copper

Mehtap Emirdag-Eanes, Banu Önen, Colin D. McMillen

PII: S0020-1693(14)00758-0
DOI: http://dx.doi.org/10.1016/j.ica.2014.12.018
Reference: ICA 16346

To appear in: *Inorganica Chimica Acta*

Received Date: 17 November 2014
Revised Date: 23 December 2014
Accepted Date: 24 December 2014

Please cite this article as: M. Emirdag-Eanes, B. Önen, C.D. McMillen, Hydrothermal synthesis and characterization of one dimensional chain structures of monolacunary Keggin polyoxoanions substituted with copper, *Inorganica Chimica Acta* (2015), doi: http://dx.doi.org/10.1016/j.ica.2014.12.018

Hydrothermal synthesis and characterization of one dimensional chain structures of monolacunary Keggin polyoxoanions substituted with copper.

Mehtap Emirdag-Eanes, [a]* *Banu Önen ,*[a] *Colin D. McMillen* [b]

[a] *Izmir Institute of Technology, Department of Chemistry Gulbahce, 35430 Izmir, Turkey*

[b] *Clemson University, Department of Chemistry, Clemson, SC, 29634, USA*

Abstract

Two novel polymeric polyoxometallates constructed from transition metal substituted heteropolytungstates, $[(4,4'bpyH_2)_2(4,4'bpyH)][PCuW_{11}O_{39}]\cdot H_2O$ (**1**), and $[(4,4'bpyH_2)(pyH)_3][PCuW_{11}O_{39}]\cdot 2H_2O$ **(2)**, (4,4'bpy = 4,4'bipyridine, py = pyridine) have been synthesized under hydrothermal conditions and characterized by IR, TGA, single crystal X-ray diffraction and magnetic measurements. The product formation showed a high sensitivity toward experimental factors including pH and stirring. Compounds **1** crystallizes in the monoclinic space group *P2(1)/n* with a = 13.503(3) Å, b = 26.726(5) Å, c = 15.168(3) Å, β = 99.61(3)° and *Z*=4. The second compound also crystallizes in space group *P2(1)/n*, but with a = 13.519(3) Å, b = 20.431(4) Å, c =18.655(4) Å, β = 96.52(3)° and *Z*=4. Compound **1** exhibits a zigzag chain structure, while compound **2** exhibits a straight chain structure. Compound **2** is the first example of a polyoxometallate containing 1D chains of transition-metal-substituted heteropolytungstate designed with two significantly different organic units as the countercations. The Cu^{2+} ions in **1** exhibit paramagnetic behavior.

Keywords: Hydrothermal, Keggin, Polyoxoanion, Hybrid, Pyridine

1. INTRODUCTION

Heteropolyanions have been studied for years and established as a large fundamental class of inorganic compounds. These anions can be viewed as molecular fragments of metal oxide clusters having a definite sizes and shapes known as polyoxometallates (POMs). [1-3] One of the first characterized examples of these discrete clusters was the Keggin polyoxoanion, which is found to exist as the classical anion $[XM_{12}O_{40}]^{y-}$ (where X is typically P, Si or B, and M = Mo or W) and several lacunary arrangements, for example, $[XM_{12}O_{39}]^{z-}$. [4] POMs have attracted great attention due to their potential applications in different areas such as catalysis, materials science and medicine. [5-9] Functionalizing polyoxometallates by adding transition metals to the Keggin structure extends their structural versatility and properties. Recently polyoxometallate-based chemistry has been enriched by hybridization with transition metal complexes and secondary transition metal substitution in the polyoxoanion (for example, $[X(TM)M_{11}O_{39}]^{n-}$, where TM = transition metal). These POMs hybridized with transition metal complexes or substituted by transition metals have received attention for their catalytic properties, [8] and may exhibit multifunctional catalysis behavior. [10] An example of the rich catalysis chemistry of one of these POMs was published by Hill and Zhang showing that α-$[PCoW_{11}O_{39}]^{5-}$ will catalyze epoxidation of alkanes. [11]

However it is only recently that a great effort has been focused on the designed synthesis of materials based on the polymerization of Keggin clusters. Strategies for synthesizing polymerized hybrid materials typically rely on 1) making indirect connections between Keggin building units where the secondary transition metal coordination complex units act as bridging ligands, or 2) linking the POMs substituted by the secondary transition metal through direct condensation to form oxo-bridged chains of Keggin clusters (through W-O-TM bridges, for example). In the first case the functionalized POM work has been highly-studied, and the POM clusters are usually observed as discrete molecules. The second case is

less studied, but many of these compounds do exhibit polymerized POM clusters by way of 1D chain structures connected through the M-O-TM oxo-bridges.[12-23] It is postulated that transition metal substituted Keggin POMs (Keggin-TPOMs) have a lower charge density on the surface than regular Keggin POMs due to the replacement of a high oxidation state metal atom with a lower oxidation state metal, [14, 24, 25] resulting in the polymerization of Keggin-TPOMs through M(VI)-O-M(II). [15, 19, 26] Several examples of these polymeric structures in the literature are found where one of the highly charged metals (W or Mo) is replaced by a lesser charged metal such as Mn^{2+} [17, 27], Cu^{2+} [19, 21, 28], Co^{2+} [18, 19], Na^{+} [29], and Ni^{2+} [16, 30], and results in polymerization by minimizing high charge density on the surface of TPOMs in comparison to discrete POM units. [12] To the best of our knowledge those monosubtituted chain-like lacunar Keggin structures that have been fully structurally characterized are summarized in Table 1.

Table 1: Chain-like Keggin structures based on $[X(M1)(M2)_{11}O_{39}]^{n-}$

Chemical formula		Reference
M2 = W		
$[ET]_{8n}[PMnW_{11}O_{39}]_n \cdot 2nH_2O$		17
$[NEt_3H]_5[XCoW_{11}O_{39}] \cdot 3H_2O$ (X=P or As)		18
$[Co(dpa)_2(OH_2)_2]_2[Hdpa][PCoW_{11}O_{39}]$		19
$[H_2bpy]_2[Hbpy][PCoW_{11}O_{39}] \cdot H_2O$		22
$[Cu(en)_2[Hen]_2[HPW_{11}CuO_{39}] \cdot 2H_2O$		16
$[Cu_4(btp)_4Cu(H_2O)_2(PW_{11}CuO_{39}] \cdot 2H_2O$		13
$[Cu^{I}(H_2O)(Hbpp)_2] \subset \{[Cu^{I}(bpp)_2[PW_{11}Cu^{II}O_{39}]\}$		15
$[PW_{11}CuO_{39}]_2 \cdot [Cu(en)_2H_2O]_4 \cdot [(CH_3)_4N]_2 \cdot 6H_2O$		12
$[Ni(DETA)_2]_3[SiNiW_{11}O_{39}] \cdot 2.5H_2O$		20
$[H_2en]_4[SiNaW_{11}O_{39}]Cl \cdot 2H_2O$		16
M2 = Mo		
$[H_2bpy][Cu(4,4'\text{-}bpy)]_2[HPCuMo_{11}O_{39}]$		14
$[(CH_3)_3NH]_{5n}[PMo_{11}MO_{39}]_n \cdot xH_2O$ (M=Mn, Co)		29
$[H_2bpy]_2[Hbpy][PCuMo_{11}O_{39}] \cdot H_2O$		21
$[H_2bpy]_2[Hbpy][PZnMo_{11}O_{39}] \cdot 2.75H_2O$		21

The Keggin chain structure was first reported by Coronado and coworkers occurring in $(ET)_{8n}[PMnW_{11}O_{39}]_n \cdot 2nH_2O$. [17] These chain structures typically feature substitutional disorder of the secondary transition metal in the Keggin anion. In some circumstances like $[ET]_8(PMnW_{11}O_{39}) \cdot 2H_2O$, the substitution clearly occurs at opposite octahedral sites on the Keggin cage as half-occupied W/Mn sites. The oxo-bridging of the POMs in the polymerized chain occurs through these sites. In the structure of $[NEt_3H]_5[XCoW_{11}O_{39}] \cdot H_2O$ (X=P or As), [18] the Co substitution is similarly localized, though at occupancy factors of 0.39 and 0.61. In other circumstances it seems likely that the secondary transition metal is disordered over all twelve possible sites or greater disorder is present amongst the POMs. [31-33] The charge on the polyoxoanion is often balanced by a series of organic countercations, most often based on a single type of organic unit. Herein we report two novel compounds having Keggin-type polyoxoanion building blocks that link directly via TM-O-W bonding to form 1D chain structures. The crystals were grown by a hydrothermal method useful for the synthesis of POMs with extended structures that are difficult to obtain under standard conditions. Characterization by X-ray diffraction, infrared spectroscopy, thermal analysis and magnetic measurements is discussed.

2. MATERIALS AND METHODS

2.1 Synthesis of $[(4,4'bpyH_2)_2(4,4'bpyH)][PCuW_{11}O_{39}] \cdot H_2O$ (1).

All chemicals were obtained commercially and used without further purification. Crystals of $[(4,4'bpyH_2)_2(4,4'bpyH)][PCuW_{11}O_{39}] \cdot H_2O$ (**1**) were synthesized using a mixture of $Na_6[H_2W_{12}O_{40}]$ (0.1 mmol, Alfa Aesar 99%), $CuCl_2 \cdot 2H_2O$ (0.5 mmol, Merck ≥ 99 %), 4,4'-bipyridine (0.5 mmol, Alfa Aesar 98 %), 7ml water and H_3PO_4 (0.3 mmol, Sigma-Aldrich, 85 %). The mixture was stirred for 1h, then transferred to a Teflon-lined autoclave (23 mL internal volume) and heated at 170° C for 3 days. After cooling to room temperature, the mixture of greenish powder, very pale blue columns and purple plate-like crystals were

filtered off, and washed with distilled water and acetone. The pale blue columnar crystals used for X-ray diffraction resulting from this hydrothermal reaction at pH 2.8 were found to be compound **1**. The other products were a mix of greenish unidentified powder and purple plates of the novel species $[Cu(4,4'bpyH)_3(4,4bpy)][HPW_{12}O_{40}]_2 \cdot 12H_2O$. [34] Compound **1** was 50% of the obtained solid product at the end of the reaction. It has been shown that the synthesis of different types of POM compounds can be quite sensitive to pH. [35] Here, synthesis was attempted at several different pH values and it is observed that even small changes of pH affect the type of the crystals obtained. Solution pH values between 2.2 and 2.7 resulted in only clear crystals of **1**, while pH values above 2.7 resulted in a mixture of **1** and the aforementioned purple side product according to Scheme 1.

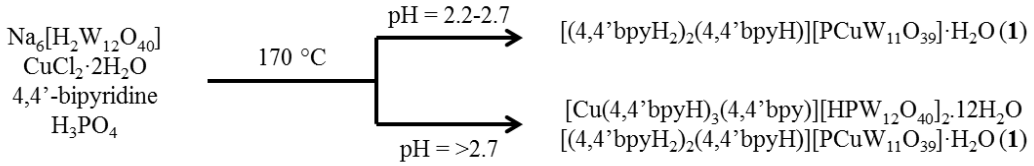

Scheme 1. Schematic illustration of the synthesis route of compound **1**.

2.2 Synthesis of $[(4,4'bipyH_2)(pyH)_3[PCuW_{11}O_{39}]\cdot 2H_2O$ (2).

All chemicals were obtained commercially and used without further purification. Crystals of $[(4,4'bipyH_2][pyH]_3[PCuW_{11}O_{39}]\cdot 2H_2O$ **(2)** were synthesized with a mixture of $Na_6[H_2W_{12}O_{40}]$ (0.1 mmol, Alfa Easer 99%), $CuCl_2\cdot 2H_2O$ (1.0 mmol, Merck ≥ 99 %), 4,4'-bipyridine (0.5 mmol, Alfa Aesar 98 %), pyridine (0.4 mmol, Merck ≥ 99 %), and H_3PO_4 (1.0 mmol, Sigma-Aldrich, 85 %). The mixture was stirred for 2 hr, then transferred to a Teflon-lined autoclave (23 mL internal volume) and heated at 170° C for 3 days. After cooling to room temperature, the products of colorless columns, pale blue diamond-shaped crystals, blue

powder and clear polycrystalline powder were filtered off, and washed with distilled water and acetone. This hydrothermal reaction yielded a very small amount of the diamond-shaped crystals of **2** and the majority product was found to be colorless columnar crystals of $[C_5NH_6]_{4.5}(H_3O)_{1.5}[P_2W_{18}O_{62}]$.[36] Compound **2** was 10% of the obtained solid product at the end of the reaction. The formation of different crystals is shown in Scheme 2. Here, we note that stirring was essential in the formation of **2**, which even then did not form in appreciable yields.

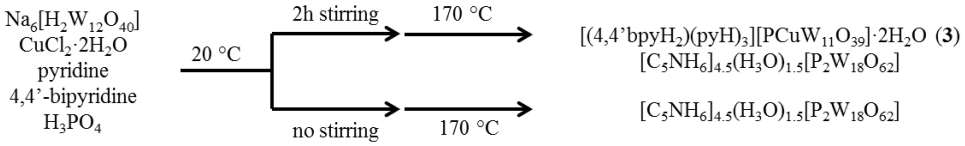

Scheme 2. Schematic illustration of the synthesis route of compound **2**.

2.3 Characterization

Infrared spectra were obtained on a Perkin-Elmer Spectrum 100 FT-IR spectrometer with KBr pellets in the 400-4000 cm^{-1} region. The thermal gravimetric analyses (TGA) of **1** were carried out using a Perkin Elmer Diamond TGA instrument. Measurements were made in flowing N_2 with a heating rate of 10° C/min for **1**. Magnetic susceptibility measurements (10-300 K) of **1** was performed using a Quantum Design Vibrating sample magnetometer.

2.4 X-Ray Crystallography

Pale blue single crystals of **1** and **2** with the dimensions of 0.33 x 0.24 x 0.24 and 0.56 x 0.14 x 0.14 respectively were carefully selected and mounted on a glass fibers. The reflection intensities of **1** and **2** were collected on a Rigaku AFC8S diffractometer with a Mercury CCD detector at 173 K using graphite-monochromated Mo Kα radiation (λ=0.71073

Å). The data were corrected for Lorentz and polarization effects using the REQAB subroutine of the *CrystalClear* software package.[37] The structures of the title compounds were solved by direct methods using SHELXL97 software and refined by using full matrix least squares on F^2. [38]All of the nonhydrogen atoms were refined anisotropically. The positions of the hydrogen atoms attached to carbon atoms were geometrically placed using a riding model, having *U*eq set at 1.2*U*eq of their assigned carbon atom. Hydrogen atoms attached to nitrogen atoms were first located using the difference map to identify which nitrogen atoms should be protonated, then similarly placed in geometrically ideal positions on those atoms. Hydrogen atoms of the water molecules in **1** and **2** were identified from the difference map, and the presence of the water molecules in all three compounds was confirmed by infrared spectroscopy (*vida infra*). Candidate tungsten atoms for the substitution with the secondary transition metals were easily identified due to their larger anisotropic displacement parameters relative to other tungsten atoms in the structures. Free refinement of the occupancies of these sites indicated very nearly half occupancy of each W and Cu. Thus the structures were modeled with these sites exactly half-occupied by each atom, and using EADP and EXYZ constraints to model the substitutional disorder. Crystallographic data for the structures reported have been deposited with Cambridge Crystallographic Data Center, CCDC deposition numbers 981289 and 981291. Crystallographic information is given in Table 2.

Table 2: Crystallographic Data and Structure Refinement

	1	**2**
Empirical Formula	$C_{30}H_{31}CuN_6O_{40}PW_{11}$	$C_{25}H_{32}CuN_5O_{41}PW_{11}$
Formula weight	3232.47	3175.42
Space group	P2(1)/n	P2(1)/n
a, Å	13.503(3)	13.519(3)
b, Å	26.726(5)	20.431(4)
c, Å	15.168(3)	18.655(4)
α, °	90	90
β, °	99.61(3)	96.52(3)
γ, °	90	90
V, $Å^3$	5397.3 (19)	5119.5 (18)
Z	4	4
D_{calc}, Mg/m^3	3.978	4.120
Parameters	803	739
μ, mm^{-1}	23.862	25.153
θ range, °	3.27-25.15	2.28-25.15
Reflections		
Collected	33766	43733
Independent	9584	9148
Observed [I≥2σ(I)]	8222	8135
R (int)	0.0717	0.0656
Final R (obs. data)[a]		
R_1	0.0734	0.0655
wR_2	0.1566	0.1567
Final R (all data)		
R_1	0.0866	0.0713
wR_2	0.1618	0.1602
Goodness of fit on F^2	1.321	1.176
Largest diff. peak, $e/Å^3$	2.974	3.068
Largest diff. hole, $e/Å^3$	-3.227	-3.103

[a] $R_1 = [\sum||F_0| - |F_c||]/\sum|F_0|$; $wR_2 = \{[\sum w[(F_0)^2 - (F_c)^2]^2]\}^{1/2}$

3. RESULTS AND DISCUSSION

3.1 Description of Structures

The title compounds, $[(4,4'bpyH_2)_2(4,4'bpyH)][PCuW_{11}O_{39}]\cdot H_2O$ (**1**), and $[(4,4'bipyH_2)(pyH)_3[PCuW_{11}O_{39}]\cdot 2H_2O$ **(2)** are novel examples of chain-like polymers of monosubstituted Keggin polyanions. The single crystal X-ray structural analysis shows that the crystals of **1** contains the $[PCuW_{11}O_{39}]^{5-}$ polyanion, $[(4,4'bpyH_2)_2(4,4'bpyH)]^{5+}$ cation units, and one water molecule. The Keggin polyoxotungstate structure is composed of 12 tungsten atoms, two of which are half-occupied by the secondary transition metals (Cu). Each W atom is six-coordinate, forming a distorted WO_6 octahedron. These are linked by both corner- and edge-sharing interactions to form four W_3O_{13} units that encapsulate a central PO_4 tetrahedron (by corner sharing W-O-P connections) as shown in Figure 1. Thus there are five different types of oxygen atoms described by their connectivities: terminal oxygen atoms bound to only one W atom (O_t), oxygen atoms shared between two tungsten atoms inside each W_3O_{13} unit (O_s), oxygen atoms shared between two tungsten atoms in different W_3O_{13} units (O_{s2}), oxygen atoms bridging between two Keggin units (O_b), and central oxygen atoms (O_c) bonded to P atoms. All the fully-occupied tungsten atoms have one short bond to a terminal oxygen atom with an average distance of 1.71(2) Å, four bonds to shared oxygen atoms (O_s and O_{s2}) ranging from 1.828(18) to 1.983(17) Å and one long bond to central oxygen atoms with the average distance of 2.42(3) Å. The central PO_4 tetrahedron exhibits an average P-O bond distance of 1.548(9) Å.

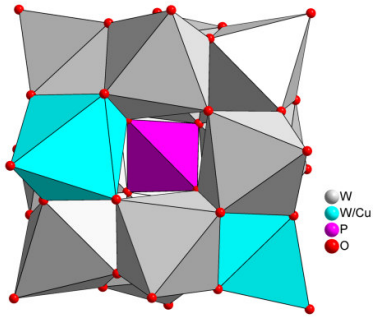

Figure 1: Polyhedral representation of Keggin polyanion in **1**.

The W/Cu mixed occupancy site present a unique connectivity in this structures. Here, the oxygen atoms that would serve as terminal oxygen atoms bound to fully-occupied W sites elsewhere in the Keggin unit instead act as bridging oxygen atoms to neighboring Keggin units. These W-O-TM bridges result in the polymerized 1D chain in this structure type. As expected, at 1.90(2) Å, the W/Cu-O_b bonds more closely resemble the W-O_s and W-O_{s2} distances than W-O_t distances. While most metal-substituted Keggins still crystallize having structures with discrete Keggin units, it should be noted that to our knowledge no 1D-chain Keggin structures have been reported to occur without M-O-TM bridging. In **1** the Keggin units propagate along [101] in a zigzag-like chain fashion (Figure 2), similar to those of the analogous monosubstituted Cu and Zn polyoxomolybdate species[21] and Co polyoxotungstate.[22] The zigzag connectivity in **1** likewise occurs since the substituted W/Cu sites are not at opposite, but rather interval positions on the Keggin unit. Alternatively, earlier reported polyoxotungstate structures exhibited straight chains where bridging oxygen atoms connect two opposite positions as in $(ET)_{8n}[PMnW_{11}O_{39}]\cdot 2nH_2O$, [17] $[NEt_3H]_5[XCo^{II}W_{11}O_{39}]\cdot 3H_2O$ [18] and $[Co(dpa)_2(OH_2)_2]_2[Hdpa][PCoW_{11}O_{39}]$. [19] Similar to the zigzag-like structure [21, 22] there is a short O···O inter-species contact between Keggin chains (2.771 Å in **1**).

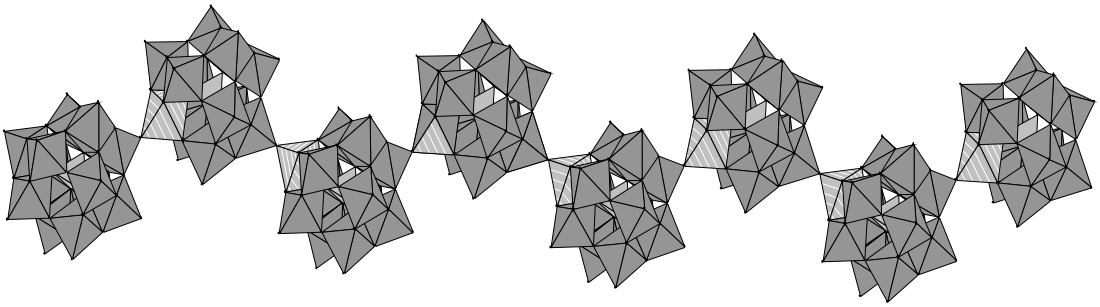

Figure 2: A polyhedral view of 1D zigzag chain in **1**. Chain propagation occurs along [101].

Voids in the extended oxide structure are filled by the crystallized water molecule as well as the one monoprotonated $(bpyH)^{+}$ and two diprotonated $(bpyH_2)^{2+}$ molecules which accomplish charge balance to the Keggin anion. Such molecules are commonly reported in the literature [11, 21, 39], and here provide important hydrogen bonding connectivity in addition to charge balance. These hydrogen bonds occur between N-H(bpy)···N(bpy), N-H(bpy)···O(polyanion), N-H(bpy)···O(water), O-H(water)···N(bpy), O-H(water)···O(polyanion) and C-H(bpy)···O(polyanion) with distances ranging from 1.933-3.043 Å. Figure 3 shows this long range structure built by some of these intermolecular contacts. There exists extensive three dimensional connectivity among the POMs by W-O-Cu, C-H···O, N-H···O and O-H···O bonding.

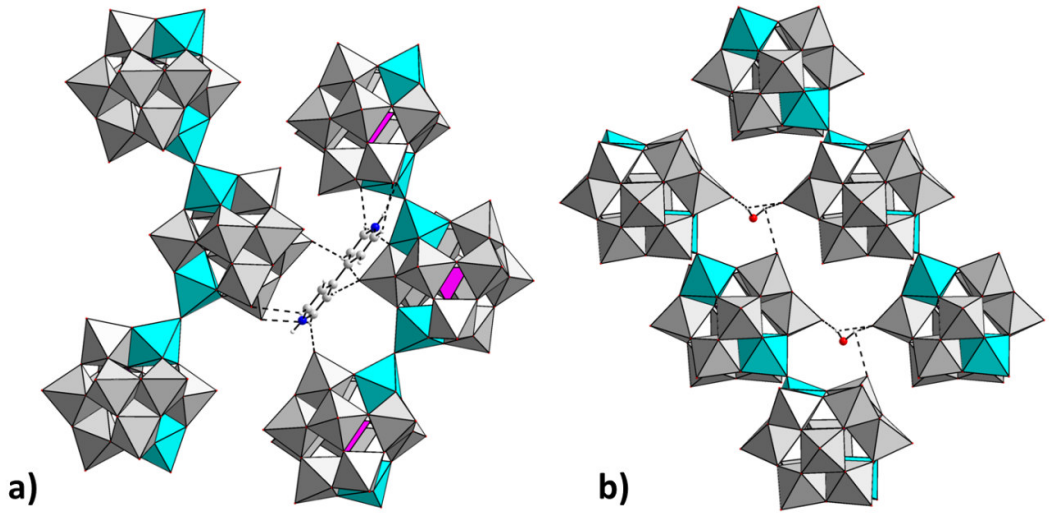

Figure 3: Selected hydrogen bonding in **1** connecting neighboring Keggin chains: a) connections along [010] by $bpyH_2$, b) connections in the *ac*-plane by H_2O.

The synthesis of compound **2** was driven by an interest to explore the versatility of the synthetic scheme to include distinctly different organic countercations (here, protonated cations of pyridine and bipyridine) and how that is manifested in the crystal structure. In doing so it was found that stirring the solution prior to hydrothermal treatment was essential in obtaining even small yields of **2**. For a solution pH of 2, stirring for two hours at 20 °C prior to hydrothermal treatment resulted in the formation of a small amount of colorless crystals of **2** as a side product to $[C_5NH_6]_{4.5}(H_30)_{1.5}[P_2W_{18}O_{62}]$ [36] when the products were harvested at the conclusion of the experiment. Compound **2** was not found to occur in any reactions that had not been stirred, which may indicate that the nucleation of **2** actually occurs while stirring at room temperature followed by modest growth under hydrothermal conditions. The nucleation and growth of $[C_5NH_6]_{4.5}(H_3O)_{1.5}[P_2W_{18}O_{62}]$ appears to be more prolific under the same conditions and is independent of stirring.

Structural analysis reveals that compound **2** also crystallizes with an infinite poly-Keggin chain, and indeed contains mixed organic countercations. The asymmetric unit of **2** contains one Keggin unit, three monoprotonated pyridines, one diprotonated 4,4'-bipyridine and two water molecules (Fig. 4). The lacunar Keggin-type $[PCuW_{11}O_{39}]^{5-}$ units are joined by W-O-Cu bridges again afforded by half occupancy of W/Cu at two sites. In contrast to **1** however, the substituted sites in **2** are opposite one another on the Keggin unit, resulting in one dimensional straight Keggin chains again propagating along [101] (Figure 5). Similar bond distances to **1** are again observed within the $[PCuW_{11}O_{39}]^{5-}$ anion of **2** (Table S1), with the average W/Cu-O_t bond length of 1.901(14) Å, again much longer than those of W-O_t bonds (1.698(15) Å) due to their bridging nature.

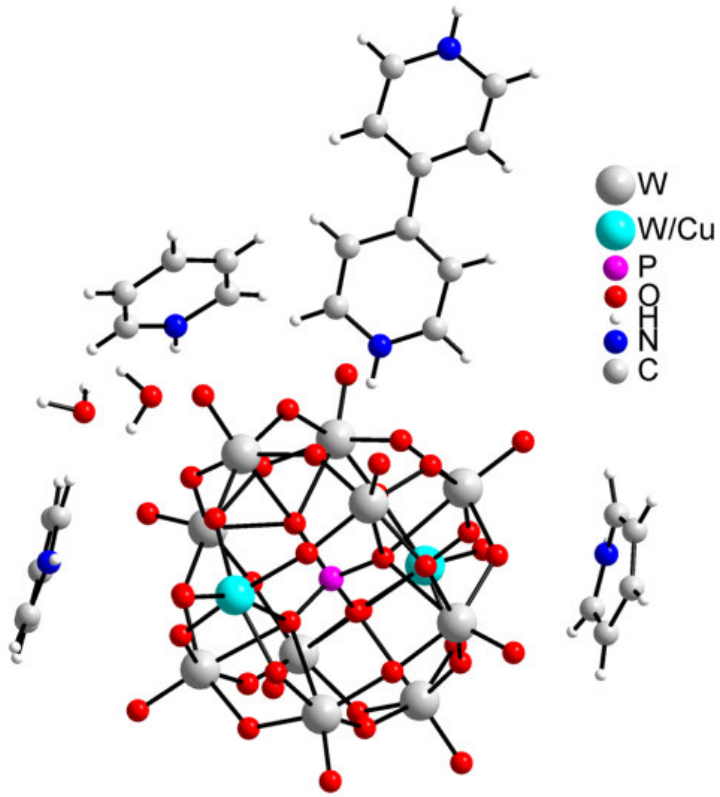

Figure 4: Asymmetric unit of **2**.

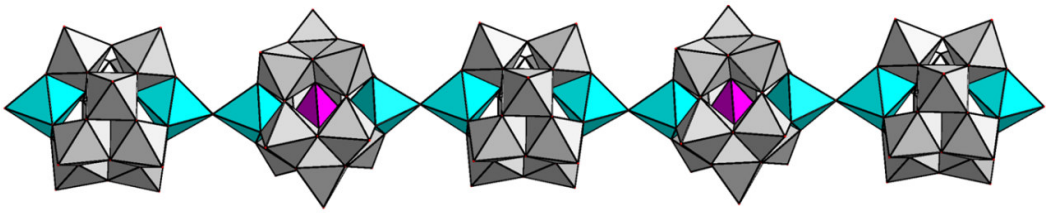

Figure 5: A polyhedral view of a 1D straight chain in **2**. Chain propagation occurs along [101].

Of particular note is that the two different organic units, $(pyH)^{+}$ and $(bpyH_2)^{2+}$ coexist in this structure to accomplish charge balance of the polyoxoanion. To our knowledge this is the first example in the literature of such mixed organic countercations with this lacunar Keggin anion. Although the ratio of starting materials in the synthesis was slightly in favor of 4,4'bipyridine, we note that there is a 3:1 ratio in favor of the pyridine units in the resulting crystal structure. Even so, this result suggests that these hydrothermal techniques could provide a rich synthetic field for varying the type and ratio of components in hybrid Keggin lattices. In **2**, the organic units and water molecules reside between the Keggin chains and connect the chains through hydrogen bonds (Figure 6). In particular, hydrogen bonding between the lattice water molecule and oxygen atoms of the POM provide connectivity along [010]. These water molecules also interact with the 4,4'bipyridine and pyridine fragments via C-H···O or N-H···O hydrogen bonding. The $bpyH_2$ unit is involved in extensive hydrogen bonding that connects POM chains in all three dimensions. The pyH units also undergo extensive hydrogen bonding providing further connectivity of POM chains in the three-dimensional supramolecular network.

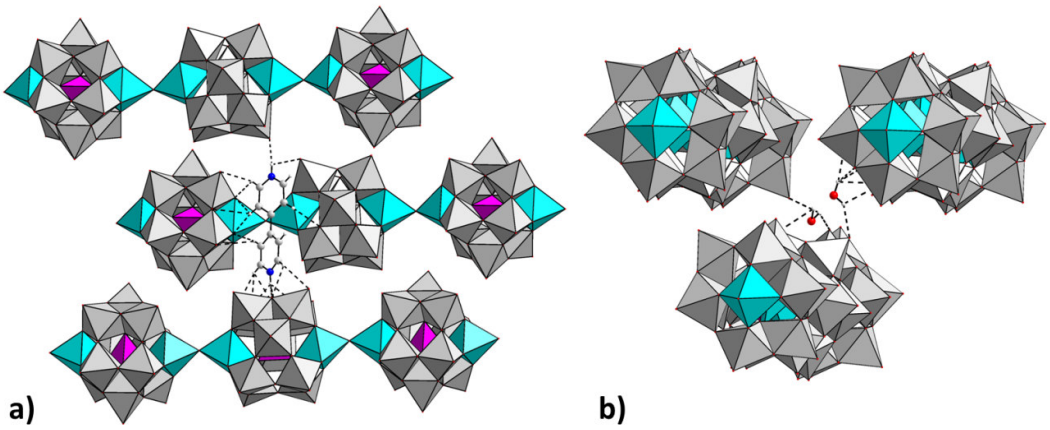

Figure 6: Selected hydrogen bonding in **2**: a) selected connectivity of a $bpyH_2$ unit (H···O bonds of 1.889(17) to 3.04(5) Å are shown as dashed bonds), b) connectivity of Keggin chains along [010] through H_2O molecules (H···O bonds of 2.080(10) to 2.724(25) Å are shown as dashed bonds).

3.2 Characterization

Infrared spectra were collected to confirm the structural features of **1-2** (Figure S1, Supporting Information). All of the spectra exhibit a series of bands in the region between 1100-1600 cm^{-1} associated with 4,4'bipyridine unit. There are also four bands characteristic of the Keggin structure. The bands centered at 1104 and 1055 cm^{-1} are attributed to P-O_c and W=O_t stretching vibrations, respectively (1085 and -982 cm^{-1} for **2**). The other two at 949 and 880 cm^{-1} for **1** can be assigned to W-O_{s2}-W and W-O_s-W bending modes, respectively (892 and 806 cm^{-1} for **2**.) (Fig. S1). The strong broad band around 3200 cm^{-1} in all the spectra is characteristic of the O-H stretching vibration of the water molecules. The substitution of W(VI) by Cu(II) in these compounds causes the slight shifts of several bands with respect to the regular Keggin units.[40]

TG curves of the title compound **1** undergo a two-step weight loss (Fig. 7). The first weight loss of 1.25 % (calcd. 0.56%) occurs between 100-340° C, and is assigned to the removal of the lattice water molecules and surface water. The second continuous weight loss of approximately 14% (calcd. 14.7%), occurs in the temperature range 340-600° C and corresponds to the release of three 4,4'bpy molecules. The weight loss progression is consistent with similar compounds in the literature [41]. Unfortunately, a suitable amount of **2** could not be obtained for characterization by thermal analysis.

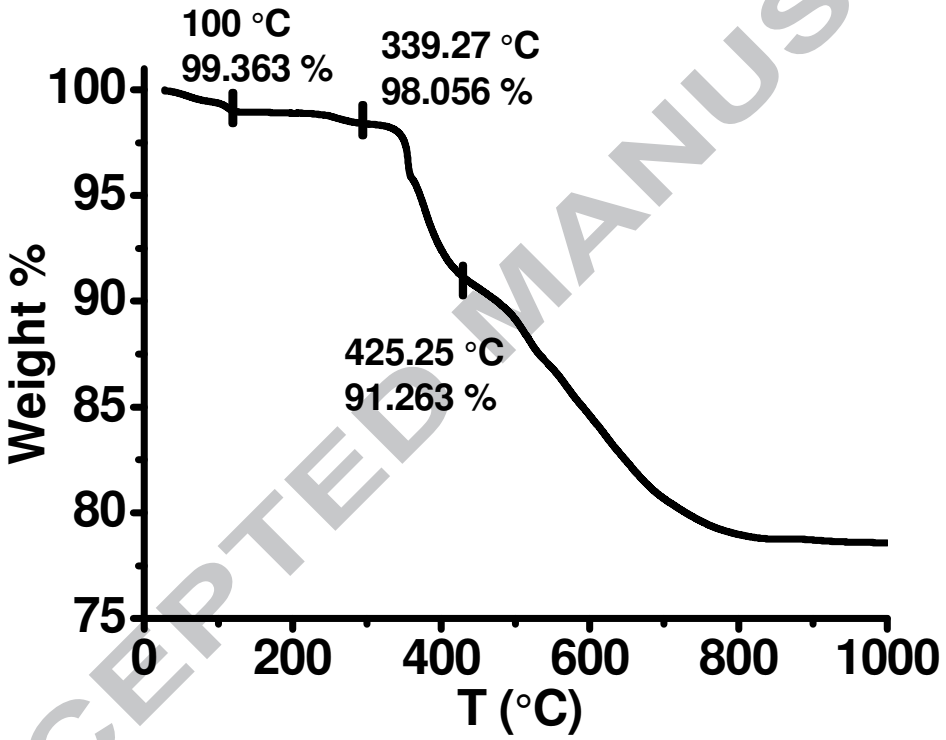

Figure 7: TGA curves of $[(4,4'bpyH_2)_2(4,4'bpyH)][PCuW_{11}O_{39}]\cdot H_2O$.

3.3 Magnetic Measurements.

The presence of Cu^{2+} ions in compound **1** motivated the study of their magnetic properties. The magnetic susceptibility of **1** was investigated on crystalline samples (7 mg) at 500 Oe between 2 and 300 K. Plots of the molar magnetic susceptibility are shown in the form of χ_M versus T (also $\chi_M T$ vs T and $1/\chi_M$ vs T) (Fig. 8). In compound **1**, Cu^{2+} ($3d^9$, S=1/2) is coordinated by six oxygen atoms from two adjacent lacunar Keggin polyanions. The W^{6+} ($3d^0$, S=0) ions do not posses an effective magnetic moment and do not contribute to the bulk properties. [27, 42] The $1/\chi_M$ versus T plots (Figure 8 insets) of **1** displays characteristic paramagnetic behavior and follow the Curie-Weiss law. Compound **1** follows the Curie-Weiss law between 10-200 K. Deviation from Curie-Weiss behavior occurs between 200-300 K for **1**, so the Curie constant (C_1= 10.1 emu K Oe^{-1} mol^{-1}) is thus derived from the $1/\chi_M$ vs T plot between 10-200 K. The magnetic moment (μ_{eff}) of **1**, determined from the equation $\mu_{eff} = 2.828 (\chi_M T)^{1/2}$ is 1.27 μ_B at 10 K, close to expected value of 1.2 for one Cu^{2+} ion. [43, 44]

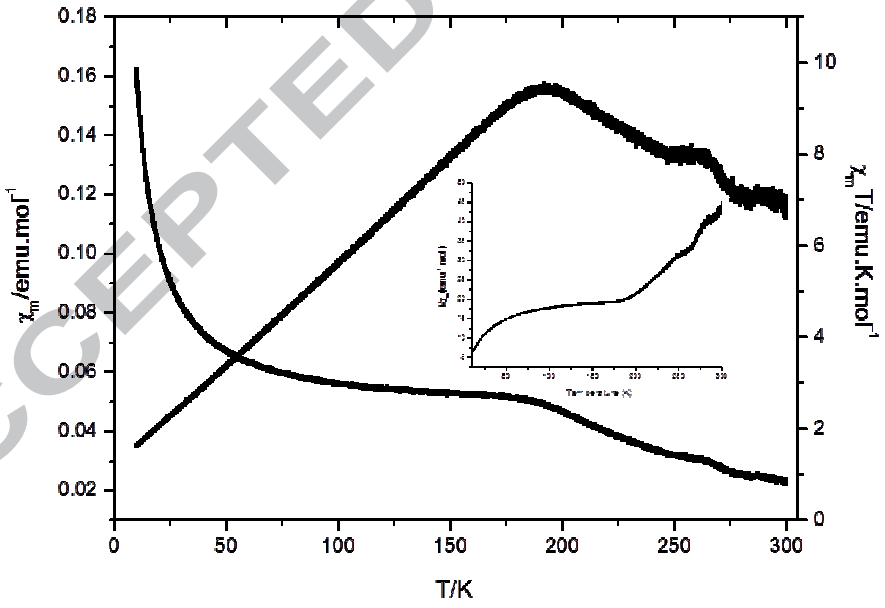

Figure 8: The temperature dependence of magnetic susceptibility χ_m and $\chi_m T$ product and inverse susceptibility (insets) for **1**.

4. CONCLUSIONS

In summary, we have synthesized and fully characterized two novel chain-like heteropolytungstates consructed by transition metal substituted Keggin units and organic units. Compound **1** shows a zigzag chain structure formed by 1D polymerized Keggin heteropolytungstate units, while compound **2** has a straight chain structure. The nature of the chain is determined by the position of the transition metal substitution in the Keggin anion. Furthermore, compound **2** is comprised of two different organic units based on pyridine and bipyridine, expanding the scope of the synthetic chemistry amongst these polyoxotungstates. It is demonstrated that the synthesis and crystal growth were significantly influenced by solution pH and stirring time. This work showed that the hydrothermal method is a powerful technique, and by changing reaction conditions a vast chemistry of POMs with different structures is accessible.

Acknowledgements

This work was financially supported by TUBİTAK (109T903). We thank Professor S. Ozcan from the department of Physics Engineering of Hacettepe University in Turkey for magnetic measurements.

Supporting Information

CCDC 981289 and 981291 contain the supplementary crystallographic data for this paper. This data can be obtained free of charge from The Cambridge Crystallographic Data Centre

via www.ccdc.cam.ac.uk/data_request/cif. Supplementary data associated with this article can be found, in the online version.

References

[1] M.T. Pope, *Heteropoly and Isopoly Oxometalates*. Springer-Verlag, Berlin, 1983.
[2] M.T. Pope, A. Muller, *Angewandte Chemie-International Edition in English* 30 (1991) 34-48.
[3] e. C. L. Hill, *Chem.Rev* 98 (1998) 1 - 387
[4] J.F. Keggin, *Proceedings of the Royal Society London A* 144 (1934) 75-100.
[5] C.Y. Sun, S.X. Liu, D.D. Liang, K.Z. Shao, Y.H. Ren, Z.M. Su, *Journal of the American Chemical Society* 131 (2009) 1883-1888.
[6] W. Qi, L.X. Wu, *Polymer International* 58 (2009) 1217-1225.
[7] Y.H. Ren, B. Yue, M. Gu, H.Y. He, *Materials* 3 (2010) 764-785.
[8] C.L. Hill, *Journal of Molecular Catalysis a-Chemical* 262 (2007) 1-1.
[9] J.T. Rhule, C.L. Hill, D.A. Judd, *Chemical Reviews* 98 (1998) 327-357.
[10] D. Hagrman, P.J. Hagrman, J. Zubieta, *Angewandte Chemie-International Edition* 38 (1999) 3165-3168.
[11] C.L. Hill, X. Zhang, *Nature* 373 (1995) 324-326.
[12] Y.H. Ren, Y.C. Hu, Z.P. Kong, M. Gu, B. Yue, H.Y. He, *European Journal of Inorganic Chemistry* (2013) 1821-1826.
[13] A.X. Tian, X.J. Liu, J. Ying, D.X. Zhu, X.L. Wang, J. Peng, *Inorganic Chemistry Communications* 14 (2011) 697-701.
[14] Y. Lu, Y. Xu, E.B. Wang, J. Lu, C.W. Hu, L. Xu, *Crystal Growth & Design* 5 (2005) 257-260.
[15] H.J. Pang, H.Y. Ma, Y. Yu, M. Yang, Y. Xun, B. Liu, *Journal of Solid State Chemistry* 186 (2012) 23-28.
[16] S. Lu, Y.G. Chen, D.M. Shi, H.J. Pang, *Inorganica Chimica Acta* 361 (2008) 2343-2348.
[17] J.R. Galanmascaros, C. Gimenezsaiz, S. Triki, C.J. Gomezgarcia, E. Coronado, L. Ouahab, *Angewandte Chemie-International Edition in English* 34 (1995) 1460-1462.
[18] H.T. Evans, T.J.R. Weakley, G.B. Jameson, *Journal of the Chemical Society-Dalton Transactions* (1996) 2537-2540.
[19] B.B. Yan, Y. Xu, X.H. Bu, N.K. Goh, L.S. Chia, G.D. Stucky, *Journal of the Chemical Society-Dalton Transactions* (2001) 2009-2014.
[20] J.Y. Niu, Z.L. Wang, J.P. Wang, *Journal of Solid State Chemistry* 177 (2004) 3411-3417.
[21] Y. Lu, Y. Xu, E.B. Wang, Y.G. Li, L. Wang, C.W. Hu, L. Xu, *Journal of Solid State Chemistry* 177 (2004) 2210-2215.
[22] J.P. Wang, Y. Shen, J.Y. Niu, *Journal of Coordination Chemistry* 60 (2007) 1183-1190.
[23] L.J. Zhang, Y.G. Wei, C.C. Wang, H.Y. Guo, P. Wang, *Journal of Solid State Chemistry* 177 (2004) 3433-3438.
[24] S.B. Li, W. Zhu, H.Y. Ma, H.J. Pang, H. Liu, T.T. Yu, *Rsc Advances* 3 (2013) 9770-9777.
[25] C.M. Liu, D.Q. Zhang, M. Xiong, D.B. Zhu, *Chemical Communications* (2002) 1416-1417.
[26] J.P. Wang, X.D. Du, J.Y. Niu, *Journal of Solid State Chemistry* 180 (2007) 1347-1352.
[27] E. Coronado, J.R. Galan-Mascaros, C. Gimenez-Saiz, C.J. Gomez-Garcia, S. Triki, *Journal of the American Chemical Society* 120 (1998) 4671-4681.
[28] L. San Felices, P. Vitoria, J.M. Gutierrez-Zorrilla, L. Lezama, S. Reinoso, *Inorganic Chemistry* 45 (2006) 7748-7757.

[29] X.Z. Liu, G.G. Gao, L. Xu, F.Y. Li, L. Liu, N. Jiang, Y.Y. Yang, *Solid State Sciences* 11 (2009) 1433-1438.
[30] L. Chen, F.L. Jiang, N. Li, W.T. Xu, M.C. Hong, *Journal of Cluster Science* 19 (2008) 591-600.
[31] V.S. Sergienko, M.A. Poraikoshits, E.N. Yurchenko, *Journal of Structural Chemistry* 21 (1980) 87-99.
[32] J. Fuchs, A. Thiele, R. Palm, *Angewandte Chemie-International Edition in English* 21 (1982) 789-790.
[33] D. Attanasio, M. Bonamico, V. Fares, P. Imperatori, L. Suber, *Journal of the Chemical Society-Dalton Transactions* (1990) 3221-3228.
[34] M. Emirdag-Eanes, B. Onen, *Inorganic Chemistry Communications* 38 (2013) 83-87.
[35] H.X. Yang, X. Lin, B. Xu, Y. You, M.N. Cao, S.Y. Gao, R. Cao, *Journal of Molecular Structure* 966 (2010) 33-38.
[36] X.L. Wang, D. Zhao, A.X. Tian, J. Ying, *Dalton Transactions* 43 (2014) 5211-5220.
[37] Rgaku/MSC, The woodlands, TX, 2009.
[38] G.M. Sheldrick, *Acta Cryst. A* 64 (2008) 112-122.
[39] C.L. Hill, R.B. Brown, *Journal of the American Chemical Society* 108 (1986) 536-538.
[40] C. Rocchicciolideltcheff, M. Fournier, R. Franck, R. Thouvenot, *Inorganic Chemistry* 22 (1983) 207-216.
[41] X.M. Lu, X.D. Shi, Y.G. Bi, C. Yu, Y.Y. Chen, Z.X. Chi, *European Journal of Inorganic Chemistry* (2009) 5267-5276.
[42] Z.G. Han, Y.L. Zhao, J. Peng, H.Y. Ma, Q. Liu, E.B. Wang, *Journal of Molecular Structure* 738 (2005) 1-7.
[43] A. Dakhlaoui, S. Ammar, L.S. Smiri, *Materials Research Bulletin* 40 (2005) 1270-1278.
[44] K. O., *Molecular Magnetism*. Wiley-VCH Weinheim, 1993.

Figure 1: Polyhedral representation of Keggin polyanion in **1**.

Figure 2: A polyhedral view of 1D zigzag chain in **1**. Chain propagation occurs along [101].

Figure 3: Selected hydrogen bonding in **1** connecting neighboring Keggin chains: a) connections along [010] by $bpyH_2$, b) connections in the *ac*-plane by H_2O.

Figure 4: Asymmetric unit of **2**.

Figure 5: A polyhedral view of a 1D straight chain in **2**. Chain propagation occurs along [101].

Figure 6: Selected hydrogen bonding in **2**: a) selected connectivity of a $bpyH_2$ unit (H···O bonds of 1.889(17) to 3.04(5) Å are shown as dashed bonds), b) connectivity of Keggin chains along [010] through H_2O molecules (H···O bonds of 2.080(10) to 2.724(25) Å are shown as dashed bonds).

Figure 7: TGA curves of $[(4,4'bpyH_2)_2(4,4'bpyH)][PCuW_{11}O_{39}]\cdot H_2O$.

Figure 8: The temperature dependence of magnetic susceptibility χ_m and $\chi_m T$ product and inverse susceptibility (insets) for **1**.

Table 1: Chain-like Keggin structures based on $[X(M1)(M2)_{11}O_{39}]^{n-}$

Chemical formula		Reference
M2 = W		
$[ET]_{8n}[PMnW_{11}O_{39}]\cdot 2nH_2O$		17
$[NEt_3H]_5[XCoW_{11}O_{39}]\cdot 3H_2O$ (X=P or As)		18
$[Co(dpa)_2(OH_2)_2]_2[Hdpa][PCoW_{11}O_{39}]$		19
$[H_2bpy]_2[Hbpy][PCoW_{11}O_{39}]\cdot H_2O$		22
$[Cu(en)_2[Hen]_2[HPW_{11}CuO_{39}]\cdot 2H_2O$		16
$[Cu_4(btp)_4Cu(H_2O)_2(PW_{11}CuO_{39}]\cdot 2H_2O$		13
$[Cu^{I}(H_2O)(Hbpp)_2]\subset\{[Cu^{I}(bpp)_2[PW_{11}Cu^{II}O_{39}]\}$		15
$[PW_{11}CuO_{39}]_2\cdot[Cu(en)_2H_2O]_4\cdot[(CH_3)_4N]_2\cdot 6H_2O$		12
$[Ni(DETA)_2]_3[SiNiW_{11}O_{39}]\cdot 2.5H_2O$		20
$[H_2en]_4[SiNaW_{11}O_{39}]Cl\cdot 2H_2O$		16
M2 = Mo		
$[H_2bpy][Cu(4,4'\text{-}bpy)]_2[HPCuMo_{11}O_{39}]$		14
$[(CH_3)_3NH]_{5n}[PMo_{11}MO_{39}]_n\cdot xH_2O$ (M=Mn, Co)		29
$[H_2bpy]_2[Hbpy][PCuMo_{11}O_{39}]\cdot H_2O$		19
$[H_2bpy]_2[Hbpy][PZnMo_{11}O_{39}]\cdot 2.75H_2O$		19

Table 2: Crystallographic Data and Structure Refinement

	1	**2**
Empirical Formula	$C_{30}H_{31}CuN_6O_{40}PW_{11}$	$C_{25}H_{32}CuN_5O_{41}PW_{11}$
Formula weight	3232.47	3175.42
Space group	P2(1)/n	P2(1)/n
a, Å	13.503(3)	13.519(3)
b, Å	26.726(5)	20.431(4)
c, Å	15.168(3)	18.655(4)
α, °	90	90
β, °	99.61(3)	96.52(3)
γ, °	90	90
V, $Å^3$	5397.3 (19)	5119.5 (18)
Z	4	4
D_{calc}, Mg/m^3	3.978	4.120
Parameters	803	739
μ, mm^{-1}	23.862	25.153
θ range, °	3.27-25.15	2.28-25.15
Reflections		
Collected	33766	43733
Independent	9584	9148
Observed [I≥2σ(I)]	8222	8135
R (int)	0.0717	0.0656
Final R (obs. data)[a]		
R_1	0.0734	0.0655
wR_2	0.1566	0.1567
Final R (all data)		
R_1	0.0866	0.0713
wR_2	0.1618	0.1602
Goodness of fit on F^2	1.321	1.176
Largest diff. peak, $e/Å^3$	2.974	3.068
Largest diff. hole, $e/Å^3$	-3.227	-3.103

[a] $R_1 = [\sum||F_0| - |F_c||]/\sum|F_0|$; $wR_2 = \{[\sum w[(F_0)^2 - (F_c)^2]^2]\}^{1/2}$

Pictogram

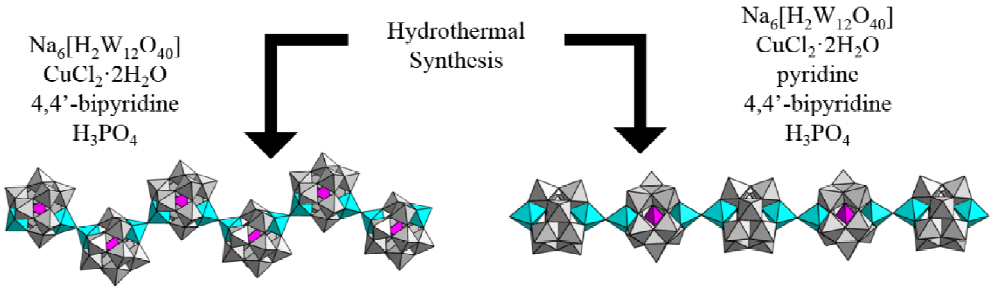

Synopsis:

Two novel hybrid POMs based on the monolacunary Keggin anion $[PCuW_{11}O_{39}]^{5-}$ have been synthesized using hydrothermal methods and characterized using X-ray diffraction, IR, TGA and magnetic methods. Keggin units propagate as 1D chains in either a straight or a zigzag fashion.

Highlights

- $[4,4'bpyH_2)_2(4,4'bpyH)][PCuW_{11}O_{39}].H_2O$ and $[4,4'bpyH_2][pyH]_3[PCuW_{11}O_{39}].H_2O$ were sythesized using hydrothermal method.
- The effect of pH of reaction media and stirring time are studied.
- Crystals were analysed using IR, TGA, magnetic measurements and x-ray diffraction.
- Molecules extends in 3D through hydrogen bonding.